Journal of Volcanology and Geothermal Research, 14 (1982) 199—222
Elsevier Scientific Publishing Company, Amsterdam — Printed in The Netherlands

ON LAVA DOME GROWTH, WITH APPLICATION TO THE 1979 LAVA EXTRUSION OF THE SOUFRIÈRE OF ST. VINCENT

HERBERT E. HUPPERT[1], JOHN B. SHEPHERD[2], HARALDUR SIGURDSSON[3] and R. STEPHEN J. SPARKS[4]

[1]*Department of Applied Mathematics and Theoretical Physics, University of Cambridge, Silver Street, Cambridge CB3 9EW (England)*
[2]*Seismic Research Unit, University of West Indies, St. Augustine (Trinidad)*
[3]*Graduate School of Oceanography, University of Rhode-Island, Kingston, RI 02881 (U.S.A.)*
[4]*Department of Earth Sciences, Downing Site, University of Cambridge, Cambridge CB2 3EQ (England)*

(Received August 9, 1981; revised and accepted February 11, 1982)

ABSTRACT

Huppert, H.E., Shepherd, J.B., Sigurdsson, H. and Sparks, R.S.J., 1982. On lava dome growth, with application to the 1979 lava extrusion of the Soufrière of St. Vincent. J. Volcanol. Geotherm. Res., 14: 199—222.

A theoretical analysis is presented for the spread of a viscous liquid flowing under its own hydrostatic pressure on a horizontal surface in order to model lava dome formation. Two situations are considered in detail: the spreading of a constant volume of liquid and the case where the amount of liquid is continually increased. Experiments with silicone liquids show close agreement with theory. The formation of a basaltic andesite lava extrusion in 1979 on the crater floor of the Soufrière of St. Vincent (West Indies) provided the motivation for and an application of the model. The extrusion reached a diameter of 868 m and a height of 133 m over a period of 150 days. Over the first 90 days the growth relationships were consistent with those predicted by theory. Application of the theory to the Soufrière dome suggests an effective viscosity of 2×10^{12} poise for the basaltic andesite lava. The large effective viscosity calculated for the lava may be attributed to the dominant influence of a high-viscosity skin which forms at the margins of the flow as it cools. After 70 days, the rate of growth of the extrusion markedly decreased because a substantial collar of rubble accumulated at the flow front. Due to this collar the growth of the extrusion ceased after 150 days. From approximately two weeks after the initiation of the extrusion, the discharge rate of lava decreased approximately linearly with increasing dome height. This observation suggests that the lava ascended under a decreasing hydrostatic driving pressure and that extrusion ceased when the lava column reached hydrostatic equilibrium.

1. INTRODUCTION

Lava domes and coulées are among the most familiar features of calc-alkaline volcanoes. The morphological characteristics of domes are often attributed to the high viscosity of the andesitic and dacitic magma which form them. More recently, it has been recognised that extrusion rate is also an important factor that controls lava shape (Walker, 1973).

In order to model the processes of dome growth we present in this paper a theoretical analysis of the radial flow of a viscous fluid on a horizontal surface. The analysis considers the change in shape of the fluid with time for two cases. First, a calculation is presented for a constant volume drop of liquid which flows under its own hydrostatic pressure. Second, a calculation is presented for a liquid continually fed onto a horizontal surface from a central source at a constant rate of influx. In this case the volume of the radially spreading drop increases linearly with time. A series of experiments was performed using two different silicone oils (13.2 and 1110 poise), the results of which agreed closely with the theoretical predictions.

During the 1971 and 1979 eruptions of the Soufrière Volcano, St. Vincent (West Indies), basaltic andesite lava extrusions were observed to form on the floor of the crater. In 1971 much of the initial growth took place underwater. However, in 1979 the crater was dry and the crater floor relatively flat and the growth of the extrusion was observed from less than 4 days after its initiation until its final explacement after five months. The spreading of the lava extrusion over the first 90 days of growth is consistent with the simple theory despite the complicating effects of cooling at the lava margin and non-Newtonian rheology. The model is used to estimate the effective viscosity of the Soufrière lava.

After August 4 (day 90) the volume of the extrusion did not change greatly. However, a small increase in diameter occurred up to October 2 (day 149) which we attribute partly to the observed avalanching of loose material from the flow front. In this later phase the behaviour of the lava clearly departed from that predicted by the viscous model. We attribute this to the increasing importance of cooling effects, notably an accumulation of a substantial collar of rubble at the flow front.

After approximately the end of May, the volume discharge rate decreased almost linearly with the height of the flow. This observation is shown to be consistent with the concept that the pressure from below, forcing the lava to erupt into the crater, was increasingly balanced by the hydrostatic pressure of the lava extrusion itself and that lava stopped flowing into the crater when the lava column reached hydrostatic pressure equilibrium.

New lava domes occur with reasonable frequency and it is hoped observations on future extrusions will be made and analysed with the current model in mind.

2. THEORY

Consider a Newtonian fluid of constant kinematic viscosity ν spreading radially on a rigid horizontal surface. Assume that the Reynolds number $R = U\,d/\nu$, where U is a representative propagation velocity and d a representative thickness of the resulting current, is sufficiently small that inertial effects can be neglected. Then the spreading occurs under the balance of two forces: the driving force proportional to the horizontal gradient of the hydrostatic pressure due to the weight of overlying fluid and the viscous retarding force.

With the co-ordinate system sketched in Fig. 1, the pressure, p, in the fluid is given by:

$$p = p_0 + \rho\, g\,(h - z) \tag{2.1}$$

where p_0 is the constant pressure at the surface, ρ is the density of the fluid and g is the acceleration due to gravity. The equation of motion of the fluid is thus:

$$\frac{1}{\rho}\frac{\partial p}{\partial r} = g\,\frac{\partial h}{\partial r} = \nu\,\frac{\partial^2 u}{\partial z^2} \tag{2.2}$$

where $u(r,z,t)$ is the radial velocity and the radial derivatives in the viscous term on the right-hand side of (2.2) have been neglected on the assumption that the thickness of the flow is very much less than its radial extent. The boundary conditions to be added to (2.2) are those of zero velocity at the bottom of the flow:

$$u(r,0,t) = 0 \tag{2.3}$$

and zero stress at the top:

$$\frac{\partial u}{\partial z}\,(r,h,t) = 0 \tag{2.4}$$

The solution of (2.2)–(2.4) is:

$$u(r,t) = \frac{1}{2}\,(g/\nu)\frac{\partial h}{\partial r}\,z(2h - z) \tag{2.5}$$

Relationships of the form (2.5) are known as lubrication theory approximations, a general discussion of which is presented in Batchelor (1967).

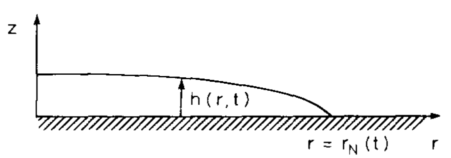

Fig. 1. The co-ordinate system used in this paper. The fluid extends radially from $r = 0$ to $r = r_N\,(t)$.

Another relationship connecting the unknowns u and h arises from the continuity equation applied on a vertical sheet of radius r in the fluid. This is:

$$\frac{\partial h}{\partial t}+\frac{1}{r}\frac{\partial}{\partial r}\left(r\int_0^h u\,\mathrm{d}z\right)=0 \tag{2.6}$$

which becomes, on substitution of (2.5):

$$\frac{\partial h}{\partial t}-\frac{1}{3}(g/\nu)\,r^{-1}\frac{\partial}{\partial r}\left(rh^3\frac{\partial h}{\partial r}\right)=0 \tag{2.7}$$

the nonlinear partial differential equation for $h(r,t)$. To (2.7) must be added a global continuity condition, such as:

$$2\pi\int_0^{r_\mathrm{N}(t)} r\,h(r,t)\,\mathrm{d}r=V \tag{2.8a}$$

if the flow results from the release of a volume V of fluid;
or

$$2\pi\int_0^{r_\mathrm{N}(t)} r\,h(r,t)\,\mathrm{d}r=Qt \tag{2.8b}$$

if a constant flux of fluid is released at a rate Q from $t = 0$;
or

$$2\pi\int_0^{r_\mathrm{N}(t)} r\,h(r,t)\,\mathrm{d}r=S\,t^{\alpha} \tag{2.8c}$$

if the volume of newly introduced fluid is given by $S\,t^{\alpha}$, where S and α are prescribed constants; or, possibly, some combination of (2.8a,b,c).

A full, general solution of (2.7) and one of (2.8) would require extensive numerical computation. Analytic solutions can be obtained, however, in terms of one similarity variable which appropriately combines r and t in such a way that (2.7) is reduced to an ordinary differential equation. Similarity solutions such as this are frequently used in fluid-mechanical investigations and tend to give accurate descriptions of the more general solutions (see, for example, Sedov, 1959; and Barenblatt, 1979). In this case, the similarity solution is expected to be valid except at the very early stages of the spreading of the flow and near the origin if fluid is being continually introduced there. The range of validity of the similarity solutions obtained will be discussed further below.

(a) Fixed volume release

Equations (2.7) and (2.8a) suggest the introduction of the similarity variable:

$$\eta = (3\nu/gV^3)^{1/8}\, r\, t^{-1/8} \tag{2.9}$$

and the solution form:

$$h = V r^{-2} H(\eta) \tag{2.10}$$

Substituting (2.9) and (2.10) into (2.7), we obtain:

$$[\eta^{-8}H^3(\eta H' - 2H)]' - \frac{1}{8}H' = 0 \tag{2.11}$$

where primes indicate differentiation with respect to η. To (2.11) must be added the boundary condition that the flow is of finite thickness at $r = 0$, and hence

$$H(0) = H'(0) = 0 \tag{2.12a,b}$$

The first integral of (2.11) which satisfies (2.12) is:

$$H^2\,(\eta H' - 2H) - \frac{1}{8}\eta^8 = 0 \tag{2.13}$$

This may be further integrated to yield:

$$H = (3/16)^{1/3}\,\eta^2\,(\eta_N^2 - \eta^2)^{1/3} \tag{2.14}$$

where η_N is the value of η at $r = r_N(t)$, the radial extent of the flow. Its value is determined from the global continuity condition (2.8a), which yields:

$$\eta_N = (1024/81\,\pi^3)^{1/8} = 0.894\ldots \tag{2.15}$$

The shape of the flow as a function of time, as given by (2.10) and (2.14), is graphed in Fig. 2. The radial extent is given by:

$$r_N = 0.894(gV^3/3\nu)^{1/8}\, t^{1/8} \tag{2.16}$$

and the height of the centre by:

$$h(0,t) = (3\nu V/4\pi g)^{1/4}\, t^{-1/4} \tag{2.17}$$

(b) Constant flux release

The appropriate similarity solution is:

$$h = (3\nu Q/g)^{1/4}\,\xi_N^{2/3}\, G(\xi/\xi_N) \tag{2.18}$$

$$\xi = (3\nu/gQ^2)^{1/8}\, r\, t^{-1/2} \tag{2.19}$$

where the introduction of ξ_N, the value of ξ at $r = r_N$, into (2.18) anticipates

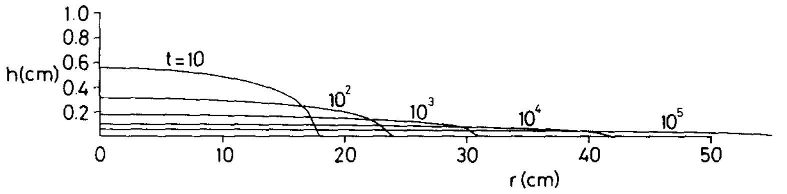

Fig. 2. The shape of a radially spreading flow for $V = 400\ \mathrm{cm}^3$, $\nu = 10\ \mathrm{cm}^2\ \mathrm{s}^{-1}$ at $t = 10, 10^2, 10^3, 10^4$ and 10^5 s.

subsequent algebraic simplification. Substituting (2.18) and (2.19) into (2.7) and (2.8b), we find that $G(x)$ satisfies:

$$(x\, G^3\, G')' + \tfrac{1}{2} x^2\, G' = 0 \tag{2.20}$$

and that ξ_N is given by:

$$\xi_N = \left(2\pi \int_0^1 x\, G\, \mathrm{d}x\right)^{-3/8} \tag{2.21}$$

Equation (2.20) needs to be solved numerically, though the first term of an expansion of G about $x = 1$:

$$G \simeq (3/2)^{1/3}\, (1 - x)^{1/3} \tag{2.22}$$

approximates G well, except near $r = 0$, where G becomes infinitely large and the model will be seen to be invalid. The numerical solution for G is graphed in Fig. 3 along with (2.22). Evaluation of (2.21) yields $\xi_N = 0.715$ (0.730 if (2.22) is used).

The shape of the flow as a function of time is presented in Fig. 4. The unboundedness of the profile at $r = 0$ is evident and is due to the similarity solution representing the introduction of a nonzero amount of fluid right on

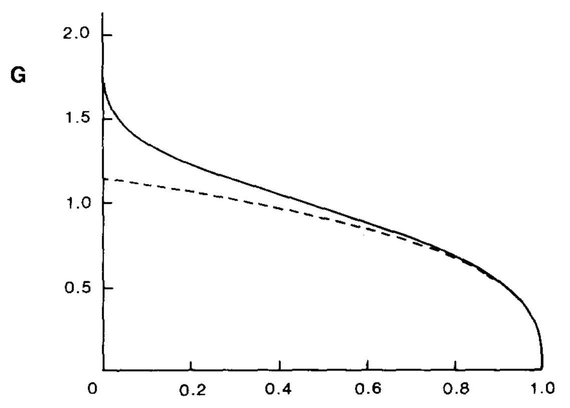

Fig. 3. Solid line: the function $G(x)$ defined by (2.20); and dashed line: (2.22), the expansion of $G(x)$ about $x = 1$.

the axis, $r = 0$, and hence introducing a singularity. Nevertheless it is expected that away from $r = 0$, the similarity solution would represent an accurate solution of the full equations. Our experiments, to be described in the next section, are consistent with this expectation. Finally, the radial extent of the flow is given by:

$$r_N = 0.715(gQ^3/3\nu)^{1/8}\, t^{1/2} \tag{2.23}$$

(c) Variable flux release

Using similar techniques to those described above, we find that the radial extent of the current is given by:

$$r_N = c(\alpha)\, (gS^3/3\nu)^{1/8}\, t^{(3\alpha + 1)/8} \tag{2.24}$$

where $c(\alpha)$ is determined from (2.8c) and is graphed in Fig. 5.

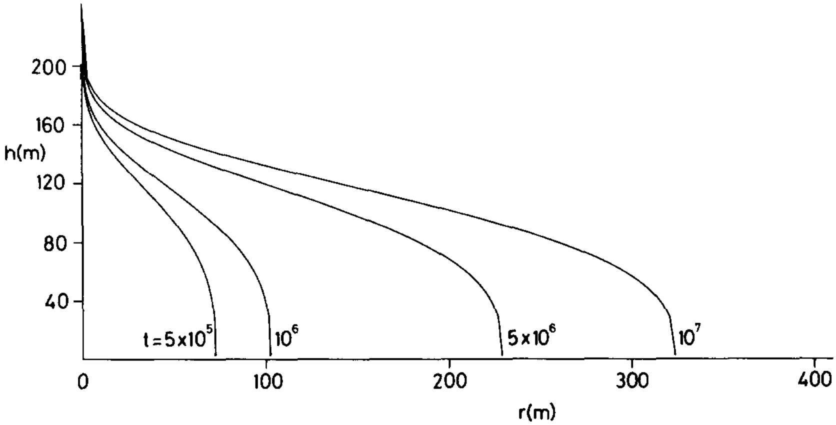

Fig. 4. The shape of a radially spreading flow for $Q = 3 \times 10^6$ cm^{3}s^{-1}, $\nu = 5 \times 10^{12}$ cm^{2}s^{-1} at $t = 5 \times 10^5$, 10^6, 5×10^6 and 10^7 s.

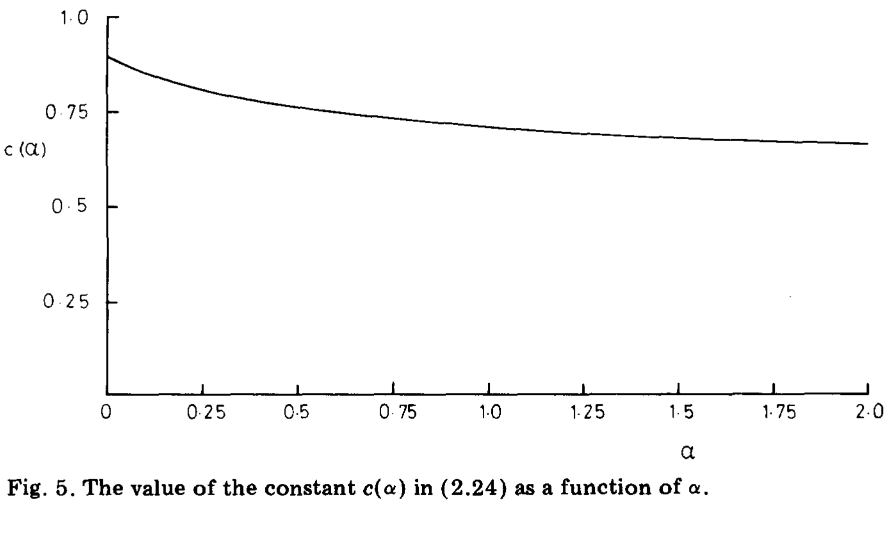

Fig. 5. The value of the constant $c(\alpha)$ in (2.24) as a function of α.

3. EXPERIMENTS

In order to examine the validity of the theoretical predictions derived in the last section, we carried out a series of laboratory experiments. Viscous fluid was allowed to spread on a five-sided sheet of Perspex. One side was 102 cm and from it two sides of 82 cm emanated at right angles. The remaining two sides were 60 cm long. An array of concentric circles of radii between 2 cm and 50 cm was inscribed on the underside of the Perspex. Before each experiment the Perspex was supported so as to be within about 0.02° of the horizontal. The Perspex was placed on a large mm ruled sheet of graph paper.

After the fluid was released, in a manner to be described below, the radial extent as a function of time was recorded. Readings at four points separated by 90° were taken and averaged to yield the values used in the analysis of the data. This method of determining the radial extent of the current allowed both small departures of the Perspex from the horizontal and effects due to the release point being off-centre to be cancelled — though for all the experiments the flow front remained quite circular.

The fluids used in the experiments were commercially available silicone oils with nominal kinetic viscosities at 25°C of 10 and 1000 cm^2s^{-1}. The exact viscosity at the laboratory temperature, $\approx 16°$, was determined by dropping a ball-bearing into the fluid contained in a measuring cylinder. From the measured terminal velocity the viscosity could be calculated as 13.2 and 1110 cm^2s^{-1} for the two oils (Table I) after making corrections for the presence of the walls of the cylinder (Happel and Brenner, § 7.3, 1965) and the nonzero Reynolds number of the flow (Van Dyke, § 1, 1975).

(a) Fixed-volume release

Five experiments were conducted. In the first two, at the start of each experiment fluid was poured near to the central point of the Perspex. In the next two, the fluid was initially held in a cylinder of radius 4.5 cm, which was raised at the start of the experiment. For the last experiment the fluid was initially confined in a Perspex cylinder with internal dimensions of $h = \frac{1}{2}(7 - r)^2$. As will be seen from the data, the mode of initiation made no difference after a few seconds from release. The height of the fluid at the central point was measured by lowering a micrometer onto the surface, though it was difficult to judge when the micrometer top was just on the surface.

Table I lists the conditions of each experiment and the best-fit parameters for the results, as defined in the caption. Figure 6 presents a plot of the results of all the experiments. With the radial extent of the flow normalised by $(gV^3/3\nu)^{1/8}$, as suggested by (2.16), all the data are seen to fall together on a universal curve. The best-fit power law through all the data is:

$$r_N = (0.887 \pm 0.002)\,(gV^3/3\nu)^{1/8}t^{0.122 \pm 0.002} \qquad (3.1)$$

TABLE I

The parameters and results of all experiments
(a) $r_N = c(gV^3/3\nu)^{1/8}t^p$, $h(0,t) = k(3\nu V/4\pi g)^{1/4}t^q$

V (cm^3)	ν (cm^{2}s^{-1})	c	p	k	q	
387	13.2	0.873 ± 0.001	0.125 ± 0.002	0.916 ± 0.027	−0.222 ± 0.009	*
933	13.2	0.860 ± 0.001	0.124 ± 0.005	1.314 ± 0.083	−0.222 ± 0.036	+
406	13.2	0.900 ± 0.000	0.120 ± 0.002	0.704 ± 0.077	−0.183 ± 0.025	×
338	1110	0.887 ± 0.000	0.122 ± 0.001	0.741 ± 0.008	−0.196 ± 0.006	□
220	13.2	0.877 ± 0.004	0.124 ± 0.002			△

(b) $r_N = K(gQ^3/3\nu)^{1/8}t^r$

Q (cm^3 s^{-1})	ν (cm^2 s^{-1})	K	r	
0.223	13.2	0.691 ± 0.010	0.501 ± 0.003	×
0.0493	13.2	0.692 ± 0.003	0.498 ± 0.001	+

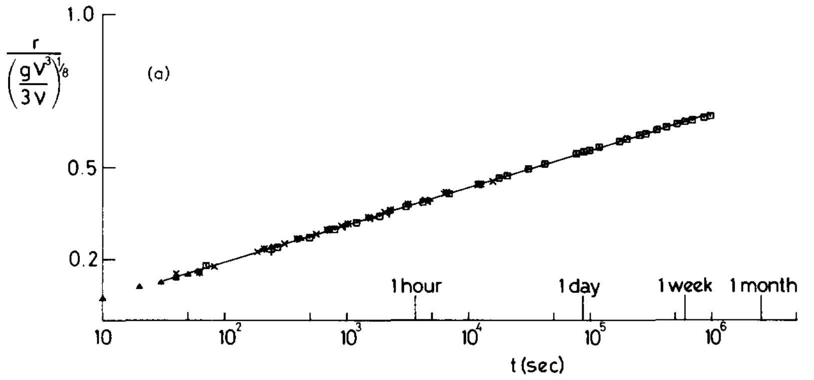

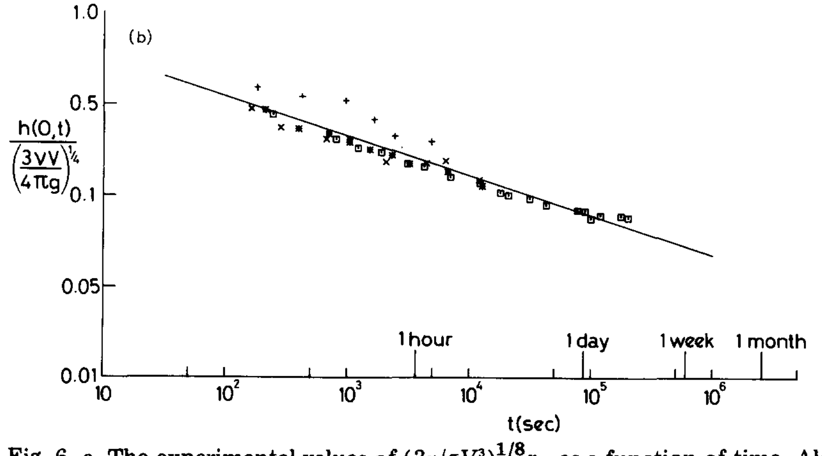

Fig. 6. a. The experimental values of $(3\nu/gV^3)^{1/8}r_N$ as a function of time. Also drawn is the best-fit power law (3.1). b. The experimental values of $(4\pi g/3\nu V)^{1/4}h(0,t)$ as a function of time. Also drawn is the best-fit power law (3.2).

The multiplicative constant and power are seen to agree well with those predicted by (2.16). The data on the height of the current at the centre is more scattered — due to the difficulty of making the measurements — though when normalised by $(3\nu V/4\pi g)^{1/4}$, as suggested by (2.17), they fall together reasonably well. The best-fit power law through all the data is:

$$h(0,t) = (0.940 \pm 0.041)\,(3\nu V/4\pi g)^{1/4} t^{0.216 \pm 0.011} \tag{3.2}$$

in reasonable agreement with (2.17).

(b) Constant flux release

Two experiments were conducted. In the first the fluid was released from a burette holding approximately 600 cm^3 maintained at a constant head and in the second from an LKB 12000 VarioPerspex pump. The conditions of both experiments and the best-fit parameters for the results are listed in Table I. Figure 7 presents a plot of all the data. The best-fit power law is:

$$r_N = (0.694 \pm 0.004)\,(gQ^3/3\nu)^{1/8} t^{0.499 \pm 0.001} \tag{3.3}$$

This is in good agreement with (2.23).

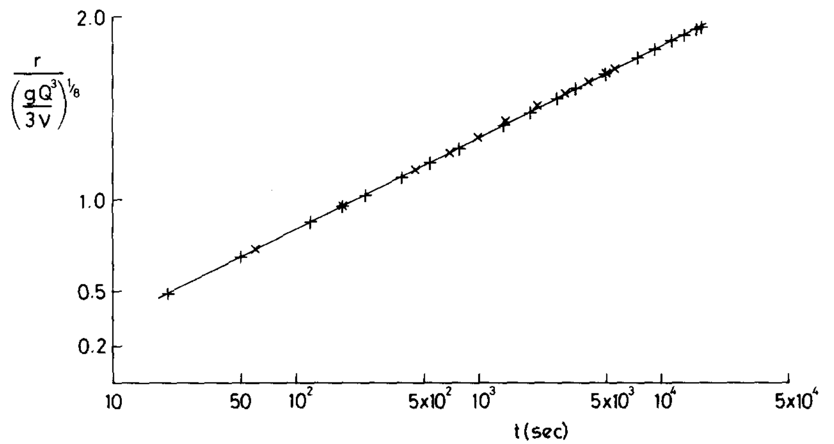

Fig. 7. The experimental values of $(3\nu/gQ^3)^{1/8} r_N$ as a function of time. Also drawn is the best-fit power law (3.3).

4. FIELD OBSERVATIONS

The Soufrière Volcano of St. Vincent in the Lesser Antilles is a 1200-m high strato-volcano with a 1.6-km diameter summit crater. During the historic period the volcano has erupted several times with notable explosive eruptions in 1718, 1812 and 1902—1903. Quieter periods of lava extrusion have also occurred with the 1971—1972 event being particularly welldocumented (Aspinall et al., 1973). The summit crater had been occupied by a 1-km diameter crater lake since shortly after the eruption of 1902—1903 but between October 1971 and March 1972 about three quarters of 7.5×10^7 m^3 of lake water evaporated as 8×10^7 m^3 of basaltic andesite lava was quietly extruded into the summit crater forming an island in the centre of the remnant lake.

The volcano remained inactive until April 13 1979 when, after over a year of mild premonitory seismic activity, explosive activity began (Shepherd et al., 1979). Between April 13 and April 26 a series of major explosions was observed forming eruption columns reaching up to 18 km in height. The explosive activity is interpreted as phreatomagmatic due to entrapment of crater lake water by ascending magma (Shepherd and Sigurdsson, 1982). When explosive activity ceased on April 26 at least 25% of the 1971—1972 extrusion had been destroyed and the crater lake no longer existed. The crater floor was dry, having been infilled with pyroclastic ejecta to about 28 m above the pre-existing lake level (680 m a.s.l.).

Between April 26 and May 3 a lava extrusion began to grow on the new crater floor. The excellent documentation of the rate and pattern of growth of this lava (Westercamp and Tomblin, 1979) provides us with an opportunity to test models for the extrusion mechanism. We cannot fix the beginning of lava growth with great precision, but it was probably no later than April 30 when a patch of rubbly material was observed in the vent at the site of the subsequent extrusion. In addition, seismic activity abruptly declined from 100 to 10 events per hour on April 30 (Shepherd and Sigurdsson, 1982). On May 3 a lava extrusion was definitely observed. On May 7 it was estimated that the height of the extrusion was 30 m and its diameter about twice as large, but since these estimates are based on visual observations and photographs from a low-flying aircraft they are subject to large errors. From May 17 onwards measurements were made from the crater rim and along 7 radial traverses across the crater floor (see Fig. 9) and the results are much more accurate. Table II gives data on the radius, height and estimated volume of the extrusion as a function of time. Figure 8 shows views of the lava extrusion at various periods during its growth and Fig. 9 shows a map of the crater and the 1979 lava. The final shape of the extrusion was lobate, with five lobes around the circumference.

The volume of the flow, to within an error of approximately 10%, is estimated by assuming that the upper surface of the lava was flat and the margins of the flow had a slope of 35°. We found that such an estimation gave results comparable to those obtained by more complicated procedures involving assumptions on the detailed flow shape. In Table II the final volume of the lava is 47.3×10^6 m^3 estimated by this method. We note that due to the lack of precision involved in estimating the volume, the increase in radius after August 14 may reflect a change in shape rather than a real change in volume.

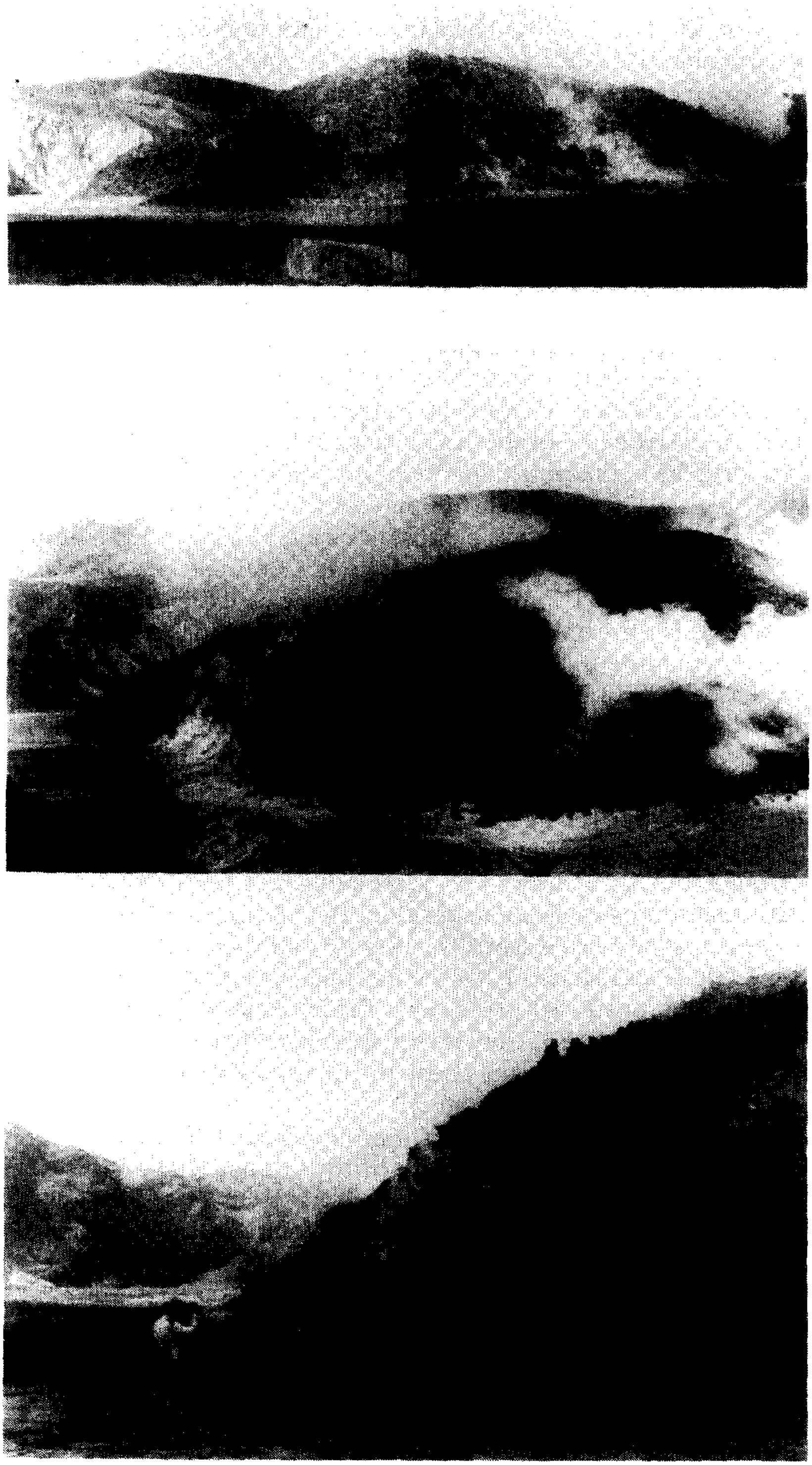

Fig. 8. Views of the Soufrière lava extrusion on August 4, 1979.

TABLE II

Data on the growth of the Soufrière lava. The values of time in days assume t = 0 on May 6 (see text for discussion)

Date	Day	Radius (m)	Height (m)	Volume (m^3)
7.5.79	1	30	30	8.5×10^4
17.5.79	8	150	69	2.3×10^6
25.5.79	19	275	82	11.9×10^6
18.6.79	43	363	100	26.2×10^6
2.7.79	57	378	117	31.2×10^6
10.7.79	65	394	117	35.0×10^6
14.7.79	69	394	120	35.4×10^6
4.8.79	90	410	123	39.5×10^6
14.8.79	100	413	131	41.4×10^6*
21.8.79	107	415	131	41.9×10^6
1.9.79	118	418	132	42.7×10^6
4.9.79	121	420	132	43.3×10^6
7.9.79	124	421	132	43.6×10^6
15.9.79	132	424	132	44.6×10^6
23.9.79	140	429	133	46.1×10^6
2.10.79	149	434	133	47.3×10^6

*The volume increase after this date may not be significant as the increase in radius could result from a change of shape at a constant volume (see text for discussion).

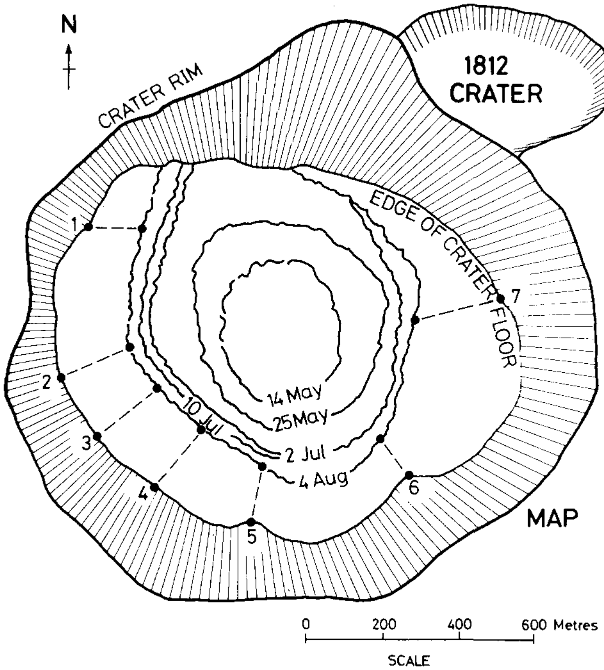

Fig. 9. Map and profile of the Soufrière crater, showing outlines of the lava extrusion at various times. The survey lines *1*—*7* were set up to measure the rate of advance of lava.

Figure 10 shows data on the diameter and height of the extrusion as a function of time. Although the longer-term average rates of expansion are smooth functions of time, there is evidence that in detail the spreading was discontinuous. For example no radial movement occurred between the 10th and 14th July (Table II) although the height of the lava increased by 3 m in the same period. The extrusion spread laterally partly by the accretion of loose, newly-cooled blocks tumbling down the flanks and partly by outward movement of whole sections of the flow-front which pushed up loose alluvial and pyroclastic material on the floor of the crater in the manner of a bull-dozer blade. To the north, lateral expansion was eventually prevented when the lava abutted against the crater wall, and the southeast and southwest expansion was restricted by remnants of the 1971—1972 lava protruding through the crater floor.

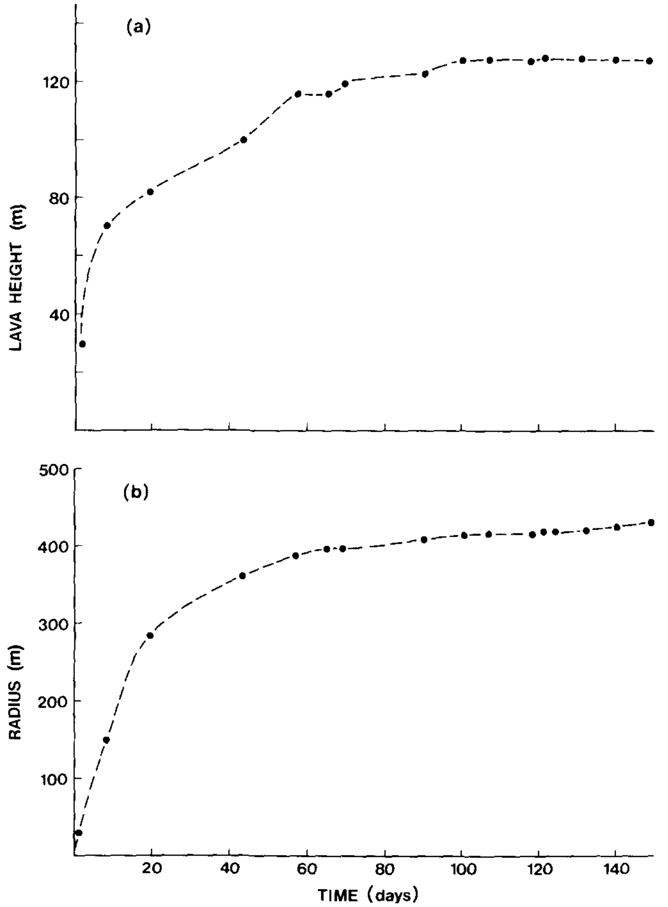

Fig. 10. a. The height of the centre of the 1979 lava above the crater floor against time. b. The radius of the lava as a function of time. After May 12 the radius is an average of seven values obtained from the survey lines (Fig. 9). For both figures t = 0 on May 6.

On October 2 the mean diameter of the lava was 868 m and the highest point above the crater floor was 133 m. The lava front sloped outwards at an angle of 30—35° (Fig. 8) to the horizontal and the top was gently convex. Even at the earliest stages of the growth of the lava the surface of the flow was disrupted into a jumble of blocks representing the cooled skin of the flow. These blocks were roughly 1 m in average diameter, but occasionally reached 4 m. Incandescence was never observed with certainty in cracks.

The lava is a basaltic andesite containing approximately 45% phenocrysts of plagioclase, clinopyroxene, orthopyroxene, titanomagnetite and minor olivine (Devine and Sigurdsson, 1983). The ground-mass of blocks sampled from the flow front consists of a dacitic glass containing quench microlites of feldspar. Table III gives major element compositions of the bulk lava and the glass. Use of the plagioclase rim-glass compositions as a geothermometer yields temperature estimates of 1100°C to 1150°C (Drake, 1976). However, petrological studies of other similar magmas and their associated nodules in the West Indies indicate temperatures of approximately 1000°C (±50°C) are more typical of basaltic andesite magmas in this arc (Arculus and Wills, 1980). The lava may also be somewhat undercooled and the plagioclase-glass pair may not be in equilibrium. A temperature in the range 800° to 1100°C is suggested in the light of the limited evidence.

TABLE III

Analytical data on 1979 lava

	1	2
SiO_2	55.03	65.90
Al_2O_3	19.42	13.70
CaO	9.25	4.05
MgO	4.32	1.23
Na_2O	3.10	3.34
K_2O	0.47	1.56
TiO_2	0.97	1.08
FeO	8.08	6.77

1. Whole-rock analysis of lava (SV-79-4) by electron microprobe analysis of fused glass.
2. Electron-microprobe analysis of glass shards (S. Carey, University of Rhode Island).

5. INTERPRETATIONS

(a) Growth rate

Figure 11 shows the volume of the lava plotted as a function of time with $t = 0$ set at May 6. The reason for this choice is that from our attempts to quantitatively understand the data, it seemed impossible to obtain general

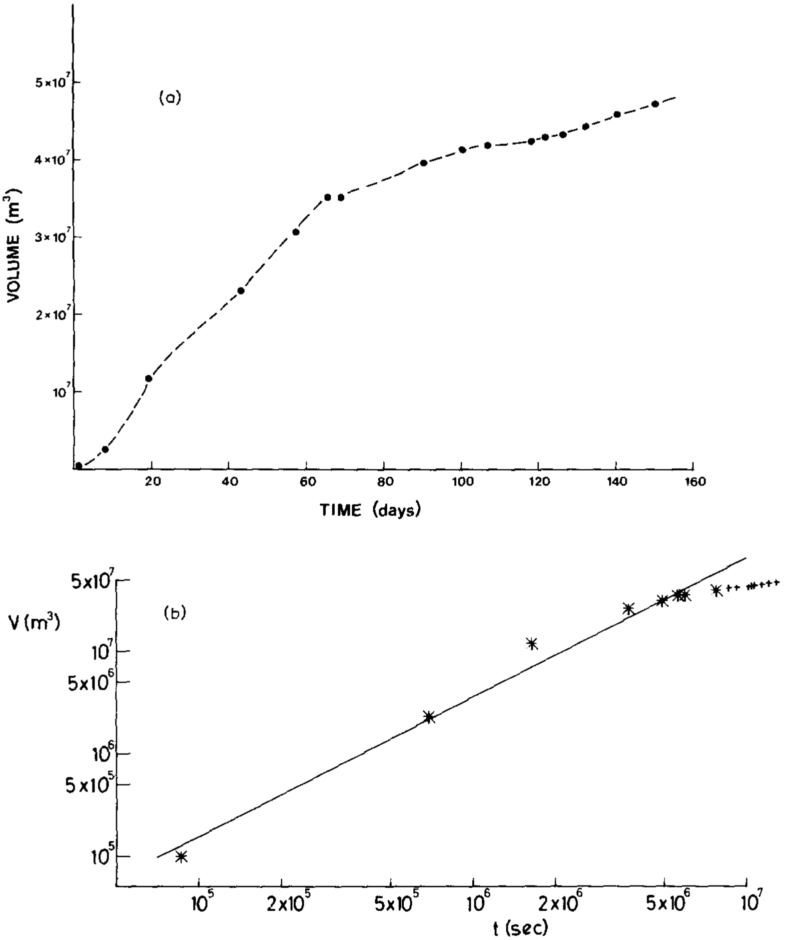

Fig. 11. The volume of the 1979 lava as a function of time.

spreading relationships which naturally included the first point (May 7) if the extrusion of lava commenced 8 days previously. However, by assuming that the extrusion started to behave as a freely flowing viscous fluid on May 6, we could obtain a quantitative description as detailed below. Although lava was first observed in the vent on April 30 the rate of discharge up to May 7 was more than an order of magnitude less than subsequent to this date. The vent was filled with ejecta and debris at this stage. We suggest that in these first few days the lava had to force its way through the vent which had been blocked by previous explosive activity. This accounts for the much reduced extrusion rate. We therefore treat the growth of the extrusion as if it began on May 6. With this supposition the data can be represented by the relationship for the first 90 days of growth:

$$V = 0.0248t^{1.36} \tag{5.1}$$

where V is the volume in m^3, t is the time in seconds and the coefficient of determination $r^2 = 0.98$. This is similar in form to (2.8c) and provides the values of the constants S and α defined in that expression.
Similarly the best-fit relationship for the lava radius is:

$$r = 0.051t^{0.58} \tag{5.2}$$

Theory would suggest from equation (2.24) that $r \propto t^{0.63}$, in reasonable agreement with the data.

(b) Lava shape

The exact shape of the flow can be obtained by numerical integration of the analogous equation to (2.20) valid for variable α. An approximate solution, which is the first term of an expansion about $r = r_N$, the front of the flow, can be readily found to be (cf. 2.22):

$$h \simeq \left[\frac{3(3\alpha+1)}{8} c^2(\alpha)\right]^{1/3} \left(\frac{3\nu S}{g}\right)^{1/4} t^{(\alpha-1)/4} \left[1-(r/r_N)\right]^{1/3} \tag{5.3}$$

This approximation suffers from the disadvantage that it underestimates the total volume in the flow (as is clearly indicated for $\alpha = 1$ in Fig. 3). This suggests that a more satisfactory approximation for the height of the current is one which has the same form as (5.3) and contains the correct total volume. This is:

$$h \simeq (14/9\pi)c^{-2}(\alpha) \left(\frac{3\nu S}{g}\right)^{1/4} t^{(\alpha-1)/4} \left[1-(r/r_N)\right]^{1/3} \tag{5.4}$$

Figure 12 compares the profile of the lava on August 4 with the profile predicted from (5.4) with $r_N = 410$ m, as suggested by the data. The theoretical shape differs from the observed shape in two ways. First, the flow front is much less steep than predicted, due to avalanching and bulldozing of sediments. Second, the height is slightly higher than predicted, which is attributed to the skin of blocks and solid material covering the surface of the flow. In general however, the fit is as good as can be expected for a first-order approximation at modelling a complex geologic body.

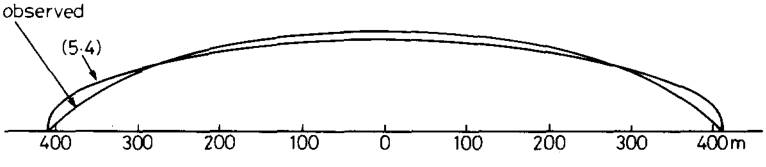

Fig. 12. A comparison of the theoretical shape of the lava according to (5.4a) and the shape of the lava on August 4.

(c) Viscosity estimates

The data on the spreading of the lava are consistent with the theoretical analysis. Thus the effective viscosity of the lava can be estimated. This is determined by the best-fit constants S and α from the data in Fig. 8 and using (2.24). The results are:

$$\begin{aligned} S &= 0.0248 \\ \alpha &= 1.36 \\ c(\alpha) &= 0.69 \\ \mu &= 2 \times 10^{12} \text{ poise} \end{aligned} \tag{5.5}$$

While the model gives a useful description of the lava's behaviour, some caution is necessary in interpreting this viscosity estimate. The basaltic andesite lava contains about 45% phenocrysts suspended in a dacitic glass. In addition, petrographic evidence shows the growth of some quench microlites during the emplacement of the flow. The temperature of the lava is estimated to be approximately 1000°C (±100°C). Table IV shows estimates for the viscosity of a liquid with composition of analysis 2 in Table III containing 45% phenocrysts in the range 700 to 1100°C. The calculations are based on work described by Shaw (1972), Shaw et al. (1968), Moore and Schaber (1975) and Pinkerton and Sparks (1978). The viscosity estimate from the fluid dynamic model is much greater than the estimates from the petrological model of viscosity in the higher temperature range and only approaches the petrological model at a temperature of 700°C. There is thus an important discrepancy in the two methods of calculation which we will consider in detail in section 6.

TABLE IV

Viscosity estimate of the Soufrière basaltic andesite lava assuming a phenocryst content of 45% and dacitic liquid phase

Temperature (°C)	Viscosity (poise)
1100	3×10^{7}
1000	2.1×10^{8}
900	2.3×10^{9}
800	3.1×10^{10}
700	8.1×10^{11}

(d) Discharge rate

Figure 13 shows the variation of volume discharge rate with height of the lava. The discharge rate is evaluated by subtracting adjacent values of the volume from Table II and dividing by the time difference. The height used is the average of the heights observed at the two adjacent times. We observe an

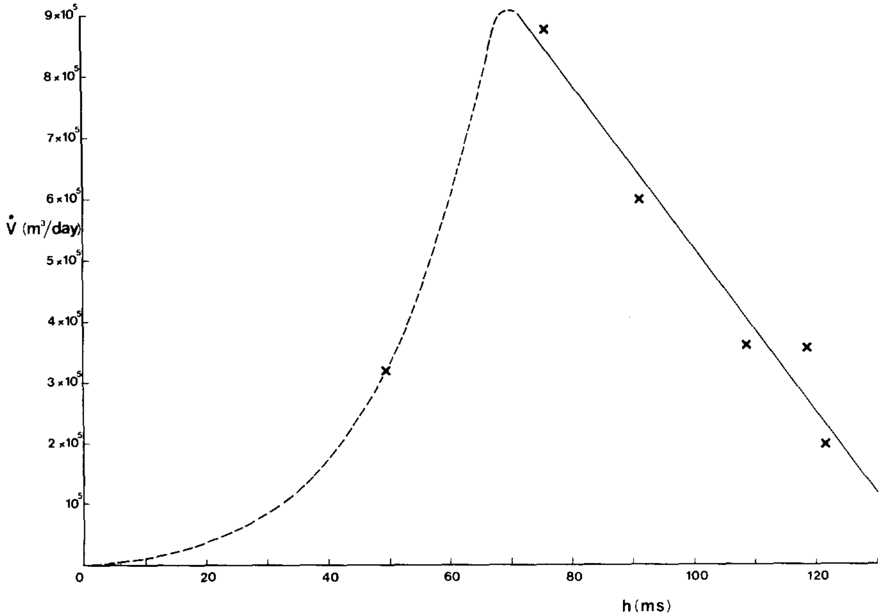

Fig. 13. Variation of volume discharge rate of lava against height.

early period when the discharge rate increased rapidly to a peak value around 105 m^3/day after a height of 75 m was reached on about May 21. Thereafter there is an approximately linear fall-off of discharge rate with increasing lava height. We suggest that this can be interpreted as due to the driving pressure in the conduit decreasing linearly with the height of the dome as the magma column approaches its equilibrium hydrostatic head. In a cylindrical volcanic conduit of diameter D the volumetric flow rate is:

$$Q = \frac{\pi D^4}{128\mu L}\,\Delta P \tag{5.6}$$

where L is the conduit length and ΔP the driving pressure. In the situation of a column of liquid rising through the crust, the value of ΔP is:

$$\Delta P = \rho_m g(h_f - h) \tag{5.7}$$

where h is the height at any given time, ρ_m is the magma density and h_f is the height of the column at which $\Delta P = 0$ and may thus be identified with the final hydrostatic height of the liquid column. This simple model predicts that:

$$Q = K(h_f - h) \tag{5.8}$$

where K is a constant which depends on the shape and length of the conduit and the magma viscosity and density. The data in Fig. 13 shows such a relationship after the lava reached a height of 69 m and supports the proposal that growth ceased when the lava column reached hydrostatic equilibrium. With the Soufrière vent positioned at the surface of the 1979 crater floor, the initial driving pressure at the crater surface is given by:

$$P = \rho_m g h \tag{5.9}$$

With $\rho_m = 2.5 \times 10^3$ kg m^{-3}, $h_f = 130$ m, (5.9) indicates that $P = 3.2$ MPa (32 bar).

For the first period of growth up to May 14 the lava increased its discharge rate rapidly. We interpret this behaviour as the result of the lava having to force its way through the conduit blocked by rubble and previously cooled lava. It appears that only after May 14 was the lava able to flow freely to the surface through an established conduit system.

6. DISCUSSION

The theoretical model for the spreading of a Newtonian fluid has been found to give good predictions for the behaviour of silicone oils in laboratory experiments. When the theory is applied to the Soufrière lava the results of the model are consistent with the observations. The prediction of the variation of spreading rate with time over the first 90 days is close to that observed. The shape of the lava is also comparable to the model except the flow front has been modified by avalanching and the height is somewhat greater than predicted.

The behaviour of the lava departs from the predicted model progressively. Specifically, the model predicts that spreading should continue indefinitely, but more and more slowly, even after the influx of lava greatly decreased in early August. The lava continued to spread after August 4 until October 2, but the field observations suggest that this was dominantly the result of avalanching at the flow front. It is possible that viscous flow was still occurring up to the beginning of October. However, after October 2 it is clear that further expansion of the flow was inhibited by some other factor, most probably the retaining strength of the flow front.

Over the first 90 days of flow the model yields an estimate of the effective viscosity of the lava of 2×10^{12} poise. This is rather higher than viscosities estimated by a petrological method (Table V) except at anomalously low eruption temperatures for a basaltic andesite lava. At least three factors might influence the value of effective viscosity: non-Newtonian properties, the effect of a cooled skin of high viscosity lava and disrupted blocks and the effects of a flow front composed of cooled lava and avalanched blocks. These are considered below.

Using the data of Pinkerton and Sparks (1978) and Moore and Schaber (1975), we estimate the yield stength of the lava to be between 500 and 10,000 Nm^{-2}. In our pure fluid model the shear stress $\mu \partial u/\partial z$ is given from (2.5) as $-\rho g \frac{h}{r}(h-z)$, which for the Soufrière lava is of order $\rho g(h-z)$. Thus

TABLE V

The depth of the solidification front at temperature T_1 as a function of time for a slab with initial temperature 1000°C, cooling by conduction

Time	T_1 = 800°C	T_1 = 900°C
1 day	0.45 m	0.54 m
10 days	1.4 m	1.7 m
100 days	4.5 m	5.4 m

the finite yield strength is exceeded within 1 m from the top of the lava, justifying the use of a Newtonian fluid model. The cooling of the upper surface of the lava can be roughly estimated by considering the cooling of a slab, initially at 1000°C, which loses heat by conduction through its upper surface that is in contact with air at 0°C. The thermal history of such a slab has been calculated by Carslaw and Jaeger (§ 11.2, I, 1959). From their analysis, the temperature profile and depth of the solidification front can be evaluated as a function of time. Table V presents the depth of the solidification front for the two cases of solidification occurring at either 800 or 900°C and incorporates a latent heat of 50 cal gm^{-1}, a specific heat of 0.3 cal gm^{-1} $°K^{-1}$ and a thermal diffusivity of 10^{-6} m^2s^{-1}. Even after 100 days the solid crust is seen to be only of the order of 5 m thick and Carslaw and Jaeger's analysis indicates that a little below this crust the lava remains close to the initial temperature. Thus a major proportion of the lava is at a uniform temperature and a uniform viscosity, justifying the use of our constant viscosity analysis.

The base of the lava will also cool, by conductive loss of heat to the crater floor, and solidify. This process, similar to that described in the preceding paragraph, merely adds a small amount of material to the floor, raising it slightly higher than the theoretical shape (Fig. 12). In detail, a slab cooling model is not directly analogous to the lava flow as the skin is being broken and stretched continually as the flow expands to form the rubbly surface. The broken nature of the surface would enhance the cooling rate whereas the thinning of the cooled skin by stretching tends to reduce the thickness of cooled material. However, cooling is still conductive and the conclusions based on the simple calculations should not be changed significantly.

Although the cooled front of the flow is thin during the active period of lava growth, we consider that the high value of effective viscosity would possibly be due to its dominant influence. At the front there will be steep thermal and therefore rheological gradients and thus a skin of high-viscosity lava will always surround the more fluid, high-temperature interior of the flow. We suggest that the effective viscosity may be due to the dominating influence of the high-viscosity flow front.

There are other situations of flow involving fluids of variable viscosity where it is the high-viscosity part of the system which controls the flow. In the case of a pipe with part of its length containing high viscosity fluid and the rest of its length containing low-viscosity fluid driven under a pressure gradient, the effective viscosity of the fluid is the mean of the two viscosities weighted by the respective lengths of the two fluids. In a lava surrounded by a skin of high viscosity it is not clear how to calculate the influence of this high viscosity because the flow pattern is very different to that in a pipe. The high value of viscosity derived from the model does suggest, however, that the viscosity at the flow front may be dominant although more data and theoretical analysis are required to verify this suggestion.

High silica melts typically change to a glass at a temperature around 700°C and at a viscosity close to 10^{13} poise (Carmichael et al., 1974). Indeed for practical purposes glass technologists often define the glass transition as the temperature at which the viscosity reaches 10^{13} poise. At lower temperatures glass will deform by brittle failure. Thus the skin of cool fluid around a silica-rich lava can be assumed to vary from some low viscosity determined by its temperature and composition to 10^{13} poise on its outer margins. Below this temperature the glassy skin will deform by tensile failure forming blocks. One possibility is that the high effective viscosity of the lava from the flow model is strongly weighted by the highest viscosity part, i.e. the marginal fluid just above the glass transition temperature. Thus the value of effective viscosity would be just beneath the glass transition temperature, in this case 2×10^{12} poise. More examples of viscous dome behaviour are needed to test this idea.

The model also does not take into account the progressive accumulation of blocks at the flow front forming a restraining collar. Even at the beginning of the lava's life the surface of the flow consisted of loose angular blocks up to 4 m in diameter. One of the most impressive features of the advance of the flow was the avalanching of these blocks from the sides of the extrusion to form a substantial scree. This scree constituted the visible flow front, which was in places pushed across the crater floor bulldozing up the crater floor sediments. There is thus an alternative view to the viscous model which is that the diminishing rate of the spreading of the lava was the consequence of the build up of a scree collar at the front of the flow of increasing size and strength.

Independent evidence for the importance of the flow front composed of rubble and cooled high viscosity lava can be found from examination of a cross-section of an older andesitic extrusion with a similar aspect ratio which is exposed in the north wall of the Soufrière crater. Figure 14a shows a geological section through the flow front. Two-thirds of the exposed section are massive, columnar jointed andesite with 57.8% SiO_2. The eastern third of the lava is the flow front and reveals a complex internal structure (Fig. 14). The flow front consists of two or three major pods of columnar rock, with jointing perpendicular to the curved cooling surface. The matrix between the massive pods and the top and bottom of the lava is composed of a mixture of angular lava blocks and scoria, similar to the surface layer of the

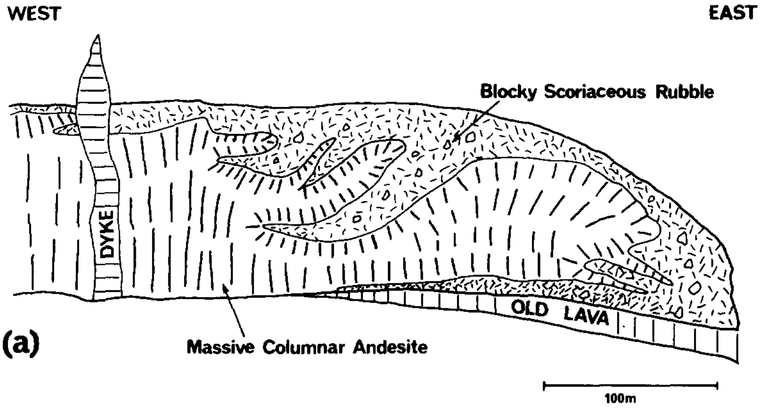

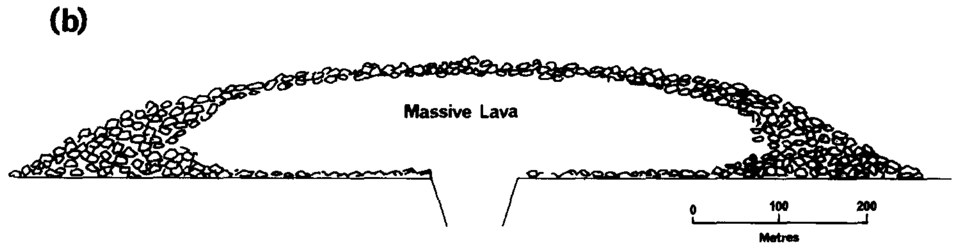

Fig. 14. a. Geological section of flow front of pre-historic andesite lava in crater wall. b. Schematic section through 1979 lava.

1979 lava. This surface layer on the pre-historic flow is of the order 5 to 10 m thick, increasing to 30 m at the snout. We consider that the structures in this pre-historic coulée provide an indication of the final internal structure of the 1979 lava extrusion. Figure 14 shows a schematic section of the structure envisaged.

If the lava flow front was sufficient to stop flow, then it may also have had significant influence earlier in the lava's growth, when the behaviour appears to be consistent with the viscous model. This will depend on how the flow front changes in size and strength with time. This is a topic which requires future investigation. We hope that the current analysis and data on the Soufrière eruption will prompt further measurements on active lava domes to test if the viscous model is an adequate treatment of growth.

ACKNOWLEDGEMENTS

R.S.J.S. acknowledges a Royal Society grant to visit St. Vincent. We thank all those who were involved in the measurements of the Soufrière lava's growth, particularly J. Tomblin, K. Rowley and W. Aspinall. We are also grateful to P.F. Linden for his aid with the laboratory experiments. This work was supported in part by the National Science Foundation grant EAR-18809. The paper is Contribution number 174 from the Department of Earth Sciences, University of Cambridge.

REFERENCES

Arculus, R.J. and Wills, K.J.A., 1980. The petrology of plutonic blocks and inclusions from the Lesser Antilles Island Arc. J. Petrol., 21: 743—799.

Aspinall, W.P., Sigurdsson, H. and Shepherd, J.B., 1973. Eruption of the Soufrière volcano on St. Vincent Island, 1971—1972. Science, 181: 117—124.

Barenblatt, G.I., 1979. Similarity, Self-similarity and Intermediate Asymptotics. Plenum Press, New York, N.Y., 218 pp.

Batchelor, G.K., 1967. An Introduction to Fluid Dynamics. Cambridge University Press, Cambridge, 615 pp.

Carmichael, I.S.E., Turner, F.J. and Verhoogen, J., 1974. Ignous Petrology. McGraw Hill, New York, N.Y., 739 pp.

Carslaw, H.S. and Jaeger, J.C., 1959. Conduction of Heat in Solids. Oxford University Press, Oxford, 510 pp.

Devine, J.D. and Sigurdsson, H., 1983. Liquid composition and crystallization history of the 1979 Soufrière magma. J. Volcanol. Geotherm. Res., in press.

Drake, M.J., 1976. Plagioclase-melt equilibria. Geochim. Cosmochim. Acta, 40: 457—465.

Happel, J. and Brenner, H., 1965. Low-Reynolds Number Hydrodynamics. Prentice-Hall, Englewoods Cliffs, N.J., 553 pp.

Moore, H.J. and Schaber, G.G., 1975. An estimate of the yield strength of the Imbrium flows. Proc. Lunar Sci. Conf., 6th, pp. 101—118.

Pinkerton, H. and Sparks, R.S.J., 1978. Field measurements of the rheology of lava. Nature, 276: 383—385.

Sedov, L.I., 1959. Similarity and Dimensional Methods in Mechanics. Academic Press, New York, N.Y., 363 pp.

Shaw, H.R., 1972. Viscosities of magmatic silicate liquids: an empirical method of prediction. Am. J. Sci., 272: 870—893.

Shaw, H.R., Peck, D.L., Wright, T.L. and Okariura, R., 1968. The viscosity of basaltic magma: an analysis of field measurements in Makaopuhi lava lake, Hawaii. Am. J. Sci., 266: 255—264.

Shepherd, J.B. and Sigurdsson, H., 1982. Mechanism of the 1979 explosive eruption of the Soufrière Volcano, St. Vincent. J. Volcanol. Geotherm. Res., 13: 119—130.

Shepherd, J.B., Aspinall, W.P., Rowley, K.C., Pereira, J.A., Sigurdsson, H., Fiske, R.S. and Tomblin, J.F., 1979. The eruption of Soufrière Volcano, St. Vincent, April—June 1979. Nature, 282: 24—28.

Van Dyke, M., 1975. Perturbation Methods in Fluid Mechanics. Parabolic Press, Stanford, Calif., 271 pp.

Walker, G.P.L., 1973. Lengths of lava flows. Philos. Trans. R. Soc. London, Ser. A, 274: 107—118.

Westercamp, D. and Tomblin, J.F., 1979. Le volcanisme récent et les éruptions historique dans la partie centrale de l'arc insulaire des Petites Antilles. Bull. B.G.R.M. (deuxieme serie), Section IV n.3/4: 293—319.